CrossMark

ORIGINAL PAPER

Rainfall variability over Alagoas under the influences of SST anomalies

G. B. Lyra[1] · J. F. Oliveira-Júnior[1] · G. Gois[1] · G. Cunha-Zeri[2] · M. Zeri[2]

Abstract The rainfall variability for the state of Alagoas, Northeast of Brazil, was evaluated based on the Standardized Precipitation Index (SPI). Harmonic decomposition was applied to 31 years-long (1960–1990) series of SPI, from 33 stations, to relate their modes of variability to El Niño-Southern Oscillation (ENSO) and the Atlantic Ocean sea surface temperature (SST). The most important harmonics identified by the spectral analysis had periods of 10–15 and 2–3 years, followed by other oscillations with smaller periods. The 10–15 years harmonic was associated with the Atlantic interhemispheric SST gradient (AITG), a cross-equatorial dipole which impacts the northeast region of Brazil by influencing the position of the intertropical convergence zone (ITCZ), leading to dry or wet conditions. The 2–3 years harmonic was consistent with the variability of ENSO events. The harmonic analysis is a powerful tool to identify the principal modes of variability of SPI. Although the magnitude of SPI is underestimated in some cases, this tool significantly increases the knowledge of the main drivers of rainfall and droughts in the region.

✉ M. Zeri
marcelo.zeri@cemaden.gov.br

G. B. Lyra
gblyra@ufrrj.br

J. F. Oliveira-Júnior
jfoliverjr@lamma.ufrj.br

G. Gois
givanildogois@gmail.com

G. Cunha-Zeri
giscunhazeri@gmail.com

[1] Departamento de Ciências Ambientais, Instituto de Florestas, Universidade Federal Rural do Rio de Janeiro, Seropédica, Rio de Janeiro 23890-000, Brazil

[2] Centro Nacional de Monitoramento e Alertas de Desastres Naturais (CEMADEN), Estrada Dr. Altino Bondensan, 500, Eugênio de Melo, São José Dos Campos, SP 12247-016, Brazil

1 Introduction

Alagoas is one of the poorest states in Brazil, and its Human Development Index (HDI) is the countrýs worst since 2000 (Malik 2013). The economy has been heavily based on the primary sector (agricultural and livestock) and the most important industry of Alagoas is processing of sugarcane, for sugar and ethanol (IBGE 2006). Considering that yields rely on the climate conditions, the characterization and trends of droughts, intense rainfalls or any other extreme climatic event is very important for both the economy and society development.

Alagoas state is located in the northeastern Brazil region (NEB), which is historically characterized by extreme climatic events, such as the drought from 1777 to 1779, when thousands died in the state of Ceará (Duarte 2001). One century later, the "three eights drought" of 1888 affected the same region leading to crop failure, cattle perishing, starvation and emigration (Gonçalves 2000). Another important drought recorded in the region occurred from 1982 to 1983, which was concomitant to the strongest El Niño event ever recorded in modern history (Molion and Bernardo 2002). Besides drought, the region is also affected by periodic floods and extreme rainfall events, like the ones in the state of Alagoas in the last century (1914, 1941, 1960, 1964, 1988, 1989, 2000), and recently in Alagoas and Pernambuco, in 2010 (Silva et al. 2010).

Rainfall over NEB is influenced by changes in atmospheric circulation and also by modes of variability of the ocean–atmosphere interactions in the Pacific and Atlantic oceans, which in general affect the region in different periods of the year (Harzallah et al. 1996; Kane 2001; Molion and Bernardo 2002; Andreoli and Kayano 2007; Cavalcanti 2012). One of those modes of variability is the El Niño-Southern Oscillation (ENSO), associated with sea surface temperature (SST) anomalies in the Central and Eastern Equatorial Pacific oceans, which influences the climate over many parts of the world and specifically the rainfall regime over NEB in interannual periods (Andreoli et al. 2004; Cavalcanti 2009; Kayano et al. 2013). While ENSO is characterized by periodic cycles of 18–36 months (Harzallah et al. 1996; Wolter and Timlin 2011), the Pacific Decadal Oscillation (PDO)—a mode of variability associated with SST anomalies over north and equatorial Pacific—has been reported to have cycles of 20–30 years (Zhang et al. 1997). Positive (negative) phases of PDO are expected to have more occurrences of intense El Niños (La Niñas) and weak and less frequent La Niñas (El Niños) (Mantua et al. 1997; Fang et al. 2008; Wang et al. 2014).

The SST of tropical Atlantic Ocean also influences rainfall over NEB via the Atlantic interhemispheric SST gradient (AITG), a cross-equatorial dipole formerly known as the Atlantic Dipole (Moura and Shukla 1981; Servain 1991; Souza et al. 1998; Souza and Nobre 1998; Servain et al. 2003). The AITG has a decadal variability (10–12 years) and impacts the northeast region by shifting the position of the Hadley cell and influencing the position of the Intertropical Convergence Zone (ITCZ). The changes in the position of ITCZ are related to the way trade winds reach NEB, enhancing or inhibiting rainfall (Moura and Shukla 1981; Harzallah et al. 1996). Finally, it has been shown that the main effects of La Niña over NEB are the passage of frontal systems over the coasts of Bahia, Sergipe and Alagoas states, and also positive anomalies of rainfall over the semiarid part of NEB (Da Silva et al. 2010). The positive anomalies are associated with the position of a Walker cell, which induces ascending and descending air, and also with the position of the ITCZ, which is modulated by the Atlantic SST (Rao and Hada 1990; Uvo et al. 1998). However, the extreme rainfall was only observed when concurrent with specific conditions of Atlantic Ocean SST: positive anomalies north of the Equator and negative anomalies south of the Equator. This result is in agreement with many other works on the teleconnection between ENSO and the Atlantic Ocean and the effects on rainfall over NEB, such as Silva et al. (2011), who have shown in a detailed observational and modeling work how different phases of PDO and ENSO interact to change rainfall patterns over South America (SA). The authors also speculate if SST anomalies over other regions,

such as the Indian Ocean, have an effect on rainfall over SA.

The most used method of assessing the severity, duration and frequency of rainfall events is through the calculation of indexes, such as the Standardized Precipitation Index (SPI) (McKee et al. 1993, 1995) or the Palmer Drought Severity Index (PDSI) (Palmer 1965; Alley 1984; Dai et al. 2004). These two indexes have been extensively used in the last decades to inform farmers and decision-makers on the severity of droughts (Alley 1984; Dai et al. 1998), on monitoring systems and forecast of crop productivity (Lohani and Loganathan 1997) and on the analysis of rainfall variability (Goyal 2014; Panthou et al. 2014). The SPI enables the assessment of severity of rainfall events in several temporal scales (e.g., monthly, bimonthly, yearly), which can later be compared with the temporal scales of climatic and weather systems influencing the region of study. Although the area of Alagoas state is small, its location over NEB enables for the identification of many weather and climate forcings that act over the region, when compared to large-scale studies (Moura and Shukla 1981; Torres and Ferreira 2011; Marengo and Bernasconi 2015). Thus, the state is representative of the main features of climate over NEB. Similar studies of SPI and harmonic analysis were done over other similarly small areas (Moreira et al. 2015), adding knowledge not only to the local context of climate, but also supporting the studies of large-scale influences of oceans over the continents (Molion and Lucio 2013; Wang et al. 2014). Finally, since SPI is a normalized index, it can be used for both humid and dry climates, requiring only that long time series (>20 years) of rainfall be used, to capture with confidence the most significant modes of variability. PDSI was not calculated in this study since it requires more data, such as air temperature, which was not available in all stations.

The atmosphere and oceans have many modes of variability (e.g., ENSO, PDO, or AITG), which evolve in time and are dependent on the chronological sequence of events. The characterization of such events can be made using time series of variables, such as air temperature and rainfall, or indices calculated from those variables. The study of time series can reveal the principal modes of variability in the past and help to predict the future values of the main variables of climate and weather (Wilks 1995). Several techniques have been used in recent years in studies of the variability of rainfall, such as harmonic and spectral analysis (Nicholson 1997; Grimm et al. 2000), wavelet transform (Penalba and Vargas 2004; Bombardi and Carvalho 2011) and gradient spectral analysis (Dantas 2008).

The relationship between extreme rainfall events in NEB and the modes of variability of ENSO and Atlantic Ocean SST anomalies have been reported in many studies in recent years (Hastenrath and Heller 1977; Alves and

Repelli 1992; Kane 2001; Andreoli et al. 2004; Andreoli and Kayano 2007; Santos et al. 2010), but with little focus on the eastern part of NEB (ENEB). The present study reports on the variability of time series of SPI over the state of Alagoas using harmonic and spectral analysis, relating the most important harmonics to known influences, such as ENSO and the Atlantic interhemispheric SST gradient.

2 Materials and methods

2.1 Characterization of the area of study

Alagoas state is located between latitudes 08°48′54″ and 10°30′09″S, longitudes 35°09′09″ and 38°15′54″W, and with altitudes lower than 850 m above sea level. The state borders the states of Pernambuco to the north and Sergipe to the South, and the Atlantic Ocean to the East. The state has 102 cities, and divided into six physiographic regions: *Zona da Mata* (humid zone), *Littoral* (coastal zone), *Sertão* (arid zone), *Sertão do São Francisco* (arid zone of São Francisco River), *Baixo São Francisco* (lowlands of São Francisco River) and *Agreste* (hinterland) (Fig. 1).

The state has a large variability in the spatiotemporal distribution of rainfall due to its topography, proximity to the ocean and the meteorological systems that affect the region. Rainfall over the state occurs mostly from April to August, characterizing the rainy season (Lyra et al. 2014). According to the Köppen climatic classification, the region's climate is of the As' type (savanna climate, with dry summer and rainy winter and autumn), observed at the humid zone, lowland São Francisco River, hinterland and part of the coastal zone. The climate type Ams' (monsoon climate, rainy winter) is observed over the northern part of the coastal zone, while the type BSs'h' and BSsh'—arid and semiarid climate—is observed over the arid zone and arid zone of São Francisco River (Gois et al. 2005).

In general, the systems that have most effect on rainfall over the state of Alagoas are trade winds, ITCZ, easterly wave disturbances, frontal systems, upper tropospheric cyclonic vortex, instability lines, mesoscale convective systems, and land and sea breezes (Hastenrath and Heller 1977; Moura and Shukla 1981; Harzallah et al. 1996; Molion and Bernardo 2002; Gois et al. 2005; Cavalcanti 2009; Lyra et al. 2014). It should be noted that several of those systems are controlled by climatological modes of
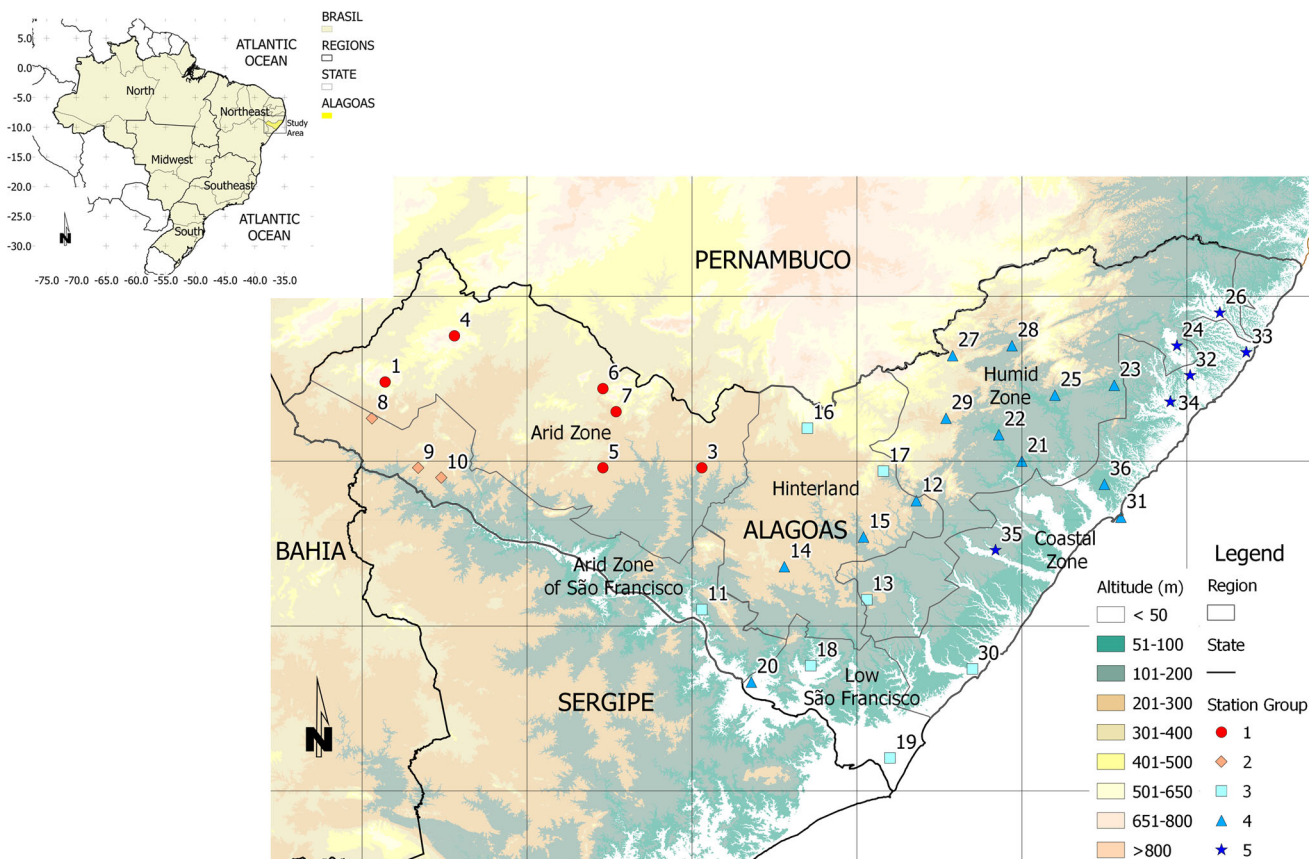
Fig. 1 Study area showing the pluviometric stations and physiographic regions of Alagoas state, with the location of the state in Brazil shown in the detail (*top left*)

variability induced by ENSO, PDO and anomalies in the SST of the Atlantic Ocean. In addition to the interannual modes of variability, such as ENSO and PDO, the region is also affected by intraseasonal and submonthly modes, such as the Madden–Julian Oscillation (MJO) (de Souza et al. 2005). The intra-annual modes of variability are beyond the scope of this paper and will be explored in a future work.

2.2 Time series of rainfall

The time series of monthly rainfall used for the calculation of SPI were obtained from a network of rain gages from *Superintendência do Desenvolvimento do Nordeste* (SUDENE), which is available at FAO ClimNet—Food and Agriculture Organization of the United Nations (FAO 2010) and *Agência Nacional de Águas* (ANA 2010). A total of 33 stations were selected based on the availability of records between 1960 and 1990, and time series of 31 years. A complete list of station's location, altitude and coordinates can be found in Lyra et al. (2014). Quality control of data was based on descriptive statistics, box plots and histograms, so that outliers could be identified and removed from the analysis. The outliers from a given station were compared to rainfall recorded at a nearby location during the same period of the year (WMO 2006). Linear regression was subsequently used to test whether each outlier was representative of the climate trends of the region (Štěpánek et al. 2009; Vicente-Serrano et al. 2010). Finally, null values were also tested against the regions' typical values and removed from the time series when inside the outliers range (Vicente-Serrano et al. 2010).

The gaps introduced by the quality control were later filled using regression analysis (Kite 1988; Allen et al. 1998; Vicente-Serrano et al. 2010). The time series were then tested for temporal homogeneity to identify sudden changes in statistical moments, such as the mean or the variance. Such a test was carried out using cumulative residuals between two nearby stations with similar rainfall patterns (Vicente-Serrano et al. 2010). The identification of stations with similar rainfall was done using clustering analysis. More details on the quality control, clustering analysis and homogeneity tests can be found in other recent studies (Lyra et al. 2006; Oliveira-Júnior et al. 2012; Lyra et al. 2014).

2.3 Standardized precipitation index

The SPI is used to quantify rainfall anomaly in different time scales using long-term records of rainfall, usually longer than 20 years (McKee et al. 1993). Here, SPI was used at the annual scale for six physiographic regions of Alagoas state. The rainfall record for each station was first fitted to a gamma distribution when the parameters of shape, α, and scale, β, were determined using the maximum verosimilarity method (MVM) (Lyra et al. 2006). Afterwards the theoretical cumulative probability $F(x)$ of a rainfall event at the annual scale was calculated according to the following expression:

$$F(x) = \int_0^x f(x)dx = \frac{1}{\Gamma(\alpha)\beta^\alpha} \int_0^x x^{\alpha-1} e^{-\frac{x}{\beta}} \mathrm{d}x \qquad (1)$$

where $f(x)$ is the probability density function and $\Gamma(\alpha)$ is the incomplete gamma function for the parameter α, i.e., no null values allowed (Thom 1958). The cumulative probability for all cases (null and not null) was calculated as:

$$F(x) = F(0) + (1 - (F(0))G(x) \qquad (2)$$

where $F(0)$ [$= m/(n+1)$] is the probability of occurrence of a null value and $G(x)$ is the cumulative distribution $F(X)$, with parameters estimated using only rainy days, where m is the rank of null values in a climatological series and n is the sample size. The cumulative distribution $F(x)$ is then transformed into a normal distribution for the random variable $Z (= (X_i - F_{50})/\sigma)$, which corresponds to the value of SPI. In the definition inside parenthesis, X_i is the annual rainfall for year i, F_{50} is the 50 % accumulated rainfall and σ is the series standard deviation. The new distribution is normal, with zero mean and standard deviation of one [$N(0,1)$].

2.4 Modes of climate variability: ENSO and Atlantic's SST anomaly

Many indices have been proposed in the literature to describe ENSO, e.g., the bivariate El Niño-Southern Oscillation (Cañón et al. 2007), the cold tongue index (Wolter and Timlin 2011), the Southern Oscillation Index (Vegas-Vilarrubia et al. 2012) and the multivariate ENSO index (MEI) (Wolter 1987), which is based on six meteorological variables measured over the tropical Pacific. These six variables are: sea level pressure, zonal and meridional components of the surface wind, sea surface temperature, surface air temperature and total cloudiness fraction of the sky. Time series of MEI were obtained from (Wolter 2016). The period was considered an El Niño year when MEI was higher than $+0.5$ for six consecutive months. Conversely, a La Niña year was assumed when MEI was lower than -0.5 for more than 6 months. If MEI was within ± 0.5 for more than 6 months, then the year was considered neutral (Rasmusson and Carpenter 1982; Cañón et al. 2007; Wolter and Timlin 2011).

The sign convention for the Atlantic interhemispheric SST gradient was that used by Menezes et al. (2008): a positive (negative) phase associated with positive (negative) anomalies of SST north of the Equator and negative

(positive) anomalies south of the Equator. Specifically, the sign is determined following this scheme: AITG is considered positive when the anomalies of North Atlantic SST (60°W–20°W, 5°N–28°N) are greater than +0.2 while the anomalies on South Atlantic (35°W–5°E, 20°S–5°N) are below −0.2. The negative phase is assumed when the signs are inverted between North and South of the Equator. The anomalies must be considered in the period from March to May, a period that was reported before to be the best for characterizing the AITG (Rao et al. 1993; Lucena et al. 2011). The phases of the Pacific Decadal Oscillation were defined based on the PDO index (Mantua et al. 1997; Zhang et al. 1997), which associates a positive (negative) phase of PDO to more occurrences of intense El Niños (La Niñas) and weak and less frequent La Niñas (El Niños). All three modes of climate variability were combined in Table 1, where events of ENSO were classified according to the phases of PDO and AITG.

2.5 Harmonic analysis

Spectral analysis makes it possible to decompose a time series into sines and cosines of different frequencies, assessing the contribution of different time scales to the variability of the signal (Wilks 1995). A time series with n elements can be represented by $n/2$ sines and cosines oscillating around the mean $\bar{y}$, as defined by the following equation:

$$
\begin{aligned}
y_i &= \bar{y} + \sum_{k=1}^{n/2} \left\{ C_k cos \left[\frac{2\pi kt}{n} - \theta_k \right] \right\} \\
&= \bar{y} + \sum_{k=1}^{n/2} \left\{ A_k cos \left[\frac{2\pi kt}{n} \right] + B_k sin \left[\frac{2\pi kt}{n} \right] \right\}
\end{aligned}
\tag{3}
$$

where k is an integer, $C_k = \left(A_k^2 + B_n^2 \right)^{1/2}$ is the amplitude, $\theta_k = arctan(B_k/A_k)$ is the phase angle, and t is the time. The value of C_k is determined as the maximum around the mean while θ_k represents the maximum of the harmonic function. The coefficients $A_k = C_k cos(\theta_k)$ and $B_k = C_k sin(\theta_k)$ were fitted to the annual values of SPI using a least-squares method.

It is not practical to use all the possible harmonics to represent the time series, since many of them cannot be distinguished from noise, and have no physical explanation. Instead, the contribution of each kth harmonic to the variance is calculated using the following equation:

$$
r_k^2 = \frac{\frac{n}{2} C_k^2}{(n-1)S_y^2}
\tag{4}
$$

where the numerator represents the sum of squares of the kth harmonic and the denominator represents the total sum of squares, with S_y^2 being the sample variance, and thus, $r^2 = \sum_{k=1}^{n} r_k^2$. Of all the n/2 harmonics which were available for the adjustment, only the first two were used, based on the value of r_k^2, since they contributed the most to the variance. Those harmonics were then referred as 'first' and 'second', sorted from high to low frequency. It should be noted that linear trends were removed the time series before the use of the harmonic decomposition, to filter out low frequencies which could not be reliably detected due to the time series length.

The spectral analysis gives information on the phase of the harmonics, measured in trigonometric degrees (0–360). When analyzing the results, phases were converted to time using the relationship between the period of the harmonic and the observed angle. Thus, an angle of 180 degrees for a harmonic of 10 years corresponded to a phase of 5 years, i.e., half the range.

3 Results and discussion

3.1 Time series of SPI: harmonic analysis

The results of harmonic analysis were evaluated by groups of stations defined previously for the state of Alagoas by Lyra et al. (2014). In that study, Ward's algorithm was used in the clustering analysis, resulting in five groups with homogeneous monthly rainfall: groups G_1 and G_2, distant ≥ 115 km from the coast, and groups G_3, G_4 and G_5, within 115 km from the coast (Fig. 1). The stations from groups

Table 1 Classification of years with ENSO events according to phases of PDO and AITG

PDO phase	Cold			Warm		
ENSO events	AITG (+)	AITG (−)	AITG neutral	AITG (+)	AITG (−)	AITG neutral
La Niña	1970	1964, 1971, 1973, 1974	1962, 1968, 1975, 1976	–	1984, 1985, 1989	1988
Neutral	–	–	1960, 1961, 1967	1978, 1979, 1980, 1981	–	1990
El Niño	1966	1965, 1972	1963, 1969	–	1986	1977, 1982, 1983, 1987

G_1 and G_2 had the lowest accumulated rainfall in the state while the largest values were recorded in the stations of groups G_3, G_4 and G_5. A positive gradient of rainfall was observed from South to North from G_1 to G_2 and from G_3 to G_5.

Two harmonics were used to characterize the variability of SPI, with their r^2 (Eq. 4) ranging from 0.28 (station 8) to 0.49 (station 1). The value of r^2 did not varied significantly within groups with homogeneous rainfall or between groups. The amplitude and phase of the first and second harmonics are shown in Figs. 2 and 3, respectively. The first harmonic with a period of 10 years was prevalent in stations of groups G_1, G_2, G_3 and G_5, except in station 17 of G_3, with period of 5 years. The harmonic of 10 years was also observed in half of stations of groups G_4. The other stations of G_4 had harmonics of 15 years (stations 12, 21, and 25) and 30 years (23, 31 and 36). Most of the stations of G_4 with periods higher than 10 years were located in the transition between the central coastal region and the northern or interior regions of the state. The influence of the 30 years harmonic and its possible relationship with the PDO could not be further explored due to the limited size of the time series used in this study.

The periods of 10 and 15 years coincide with the period of oscillation of the AITG, which is 10–12 years (Chang et al. 1997). In addition, it has been reported a variability of 13–14 years of rainfall over north of NEB, associated with the adjacent equatorial Atlantic, as well as a variability of 27–28 years, which was associated with the 30 years

oscillation of PDO (Hastenrath 2012). Finally, the interannual variability (2–5, 5–7 years) and decadal variability (15–22 years) were found to be related to ENSO and the PDO, respectively, in a study over the Zona da Mata and Central Coastal region of Alagoas (Silva et al. 2009, 2010).

The second strongest harmonic for most of the stations (≈ 88 %) had a period of 2.3 or 2.7 years (Fig. 3). The exceptions were stations 9 and 10 (period of 2.1 years) and stations 7 and 11 (period of 3.8 years). This harmonic was most likely influenced by ENSO events, which are known to affect this region and to have periods of oscillation of 1.5–3 years (Harzallah et al. 1996; Wolter and Timlin 2011). It follows that the influence of ENSO over the state is much stronger and spatially homogeneous in comparison with the first harmonic, as it is evident by the higher amplitude of the second harmonic, denoted by the arrows size, and the dominant phase angle of ≈ 135 degrees throughout the state.

The adjustment of the first harmonic to the time series of SPI was successful, since it matched the occurrence of the majority of events (more than 80 % of agreement). However, ≈ 10 % of events occurred in disagreement with the expected value, such as the drought of 1976 recorded in stations 1–4, and 8–10, which occurred in a period when SPI was expected to be positive according to the trends of the first harmonic. The matching of the first two harmonics to the SPI sign was also successful (54.8 %, in station 30, to 90.3 % in station 12). The harmonics had amplitudes between -1.24 and 1.24, which corresponds to moderate
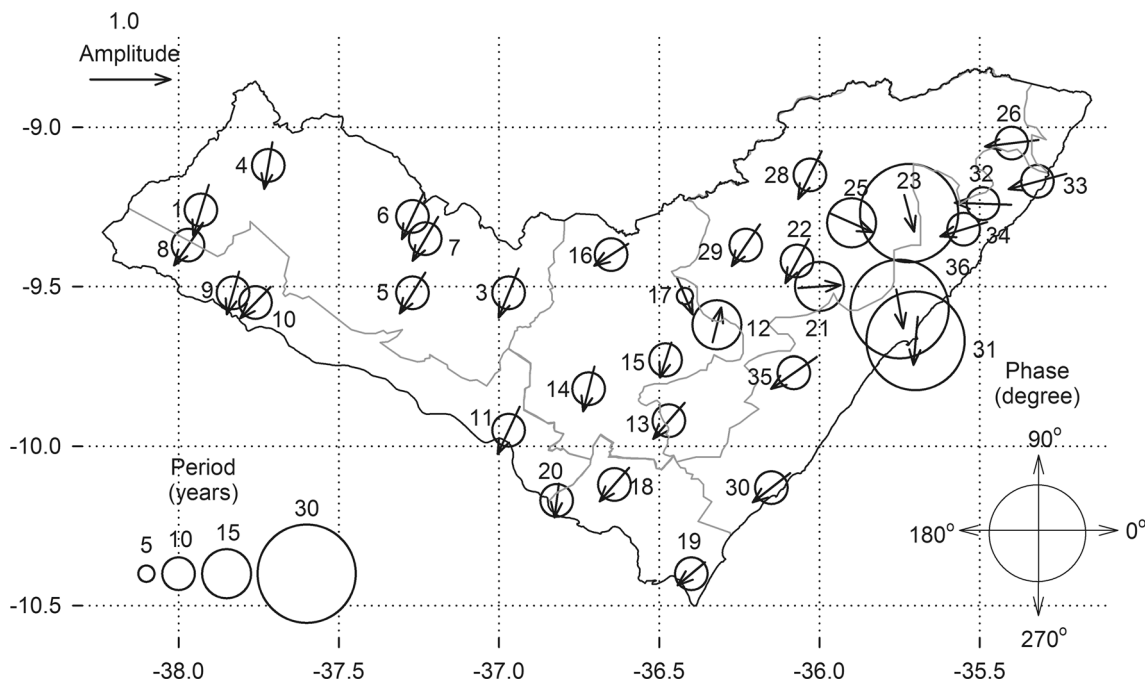
Fig. 2 Period, amplitude and phase angle for the first harmonic applied to SPI data
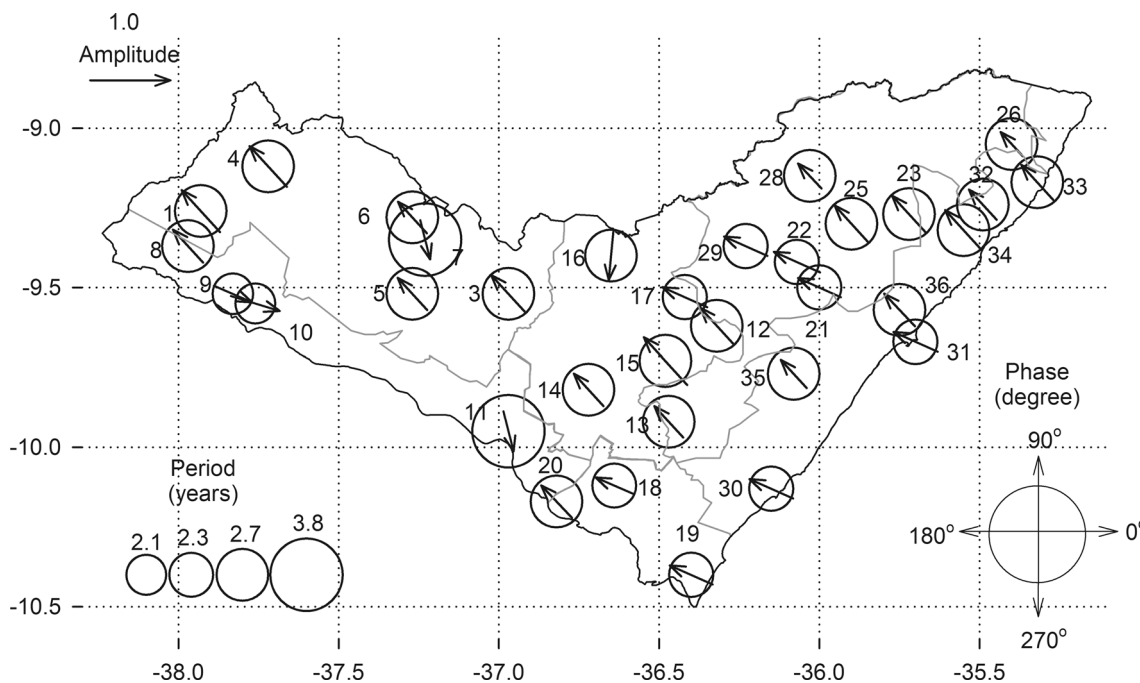
**Fig. 3** Similar to Fig. 2, but for the second harmonic

dry and moderate wet periods, resulting in r^2 lower than 0.5 when accounting for the variance of SPI explained by the harmonics. A certain degree of disagreement was expected, since the adjustment of the harmonics is based on a mean agreement with the time series, which finally leads to better adjustment in some periods and more disagreement with the data in other parts of the time series. While the sines and cosines in the harmonic analysis are periodic and infinite, the real oscillations in the time series change over time, either to higher or lower frequencies. For example, the decadal oscillation of the AITG started in the 70 s and was not evident before that (Servain 1991).

3.2 SPI and climate variability modes

The harmonics described in this work were similar to the ones found in a study of the variability of rainfall over NEB (Harzallah et al. 1996). The work had an observational component, using data from 1970 to 1988, and a statistical part, using the singular value decomposition method. The study area ranged from 36°W to 43°W, and from 2°S to 12°S, an extensive region which includes NEB. The first oscillation found in that study was related to ENSO and the North Atlantic Subtropical High, which influenced the zonal circulation, and thus, the position of a Walker cell over the region. The second oscillation had a period of approximately 10 years, which was associated to the AITG and influenced the meridional tropical circulation and the position of a Hadley cell.

From a total of 33 stations, 26 (~79 %) had the first harmonic of 10 years, while harmonics of 5, 15 and 30 years were present in 1, 3 and 3 stations, respectively. While describing the results, the stations can be evaluated into three patterns based on the first harmonic. The first pattern includes the majority of stations (22), which are located all over the state including the arid zone (G_1 and G_2), hinterlands, the transition to the coast, and the southern part of the coastal region (G_3 and G_4) (Figs. 4, 5, 6). According to Fig. 2, those stations have a phase angle of ~240°, which corresponds to a phase of between 6 and 7 years. The similar phase throughout the state suggests that the decade-long influence on rainfall is registered simultaneously over an extensive area, due to the large-scale nature of the influence of the AITG. The absolute value of this phase is more important when compared to the phases in other regions.

Based on the periods identified by the first harmonic, a pattern was established between the phases of PDO (cold and warm), the values of SPI and the sign of AITG and ENSO. When PDO was cold (1960–1976), SPI, AITG and ENSO were *positively* correlated, i.e., years with negative SPI (1960–1964 and 1970–1974) (Figs. 4, 5, 6) were more frequent (>80 % of years) when AITG index and ENSO were *negative* (Table 1), and vice versa for positive values (1965–1969 and 1975/76). Conversely, when PDO was warm (1977–1990), the relationship was characterized by a *negative* correlation between SPI, AITG and ENSO, i.e., years with negative values of SPI (1980–1984 and
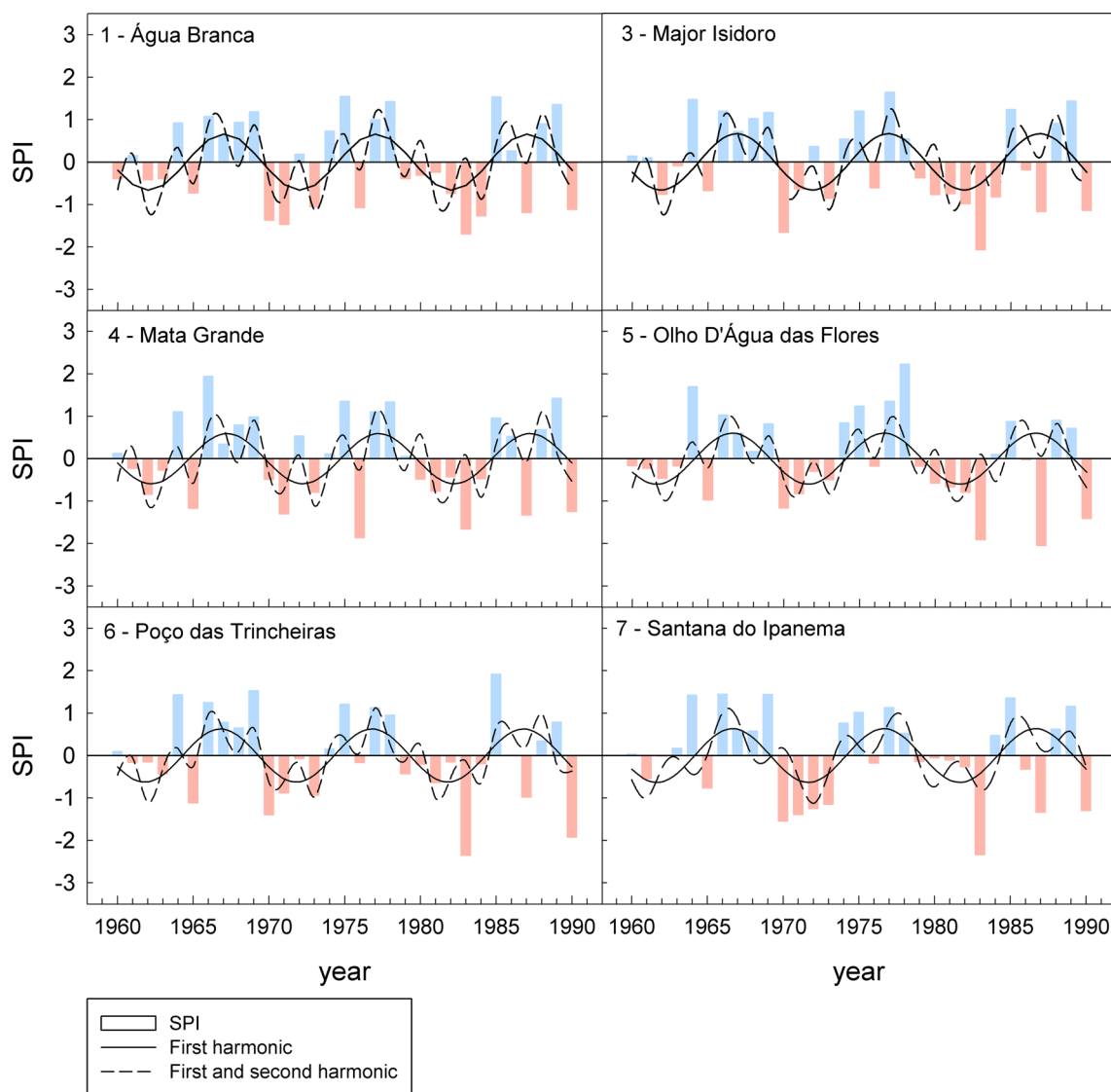
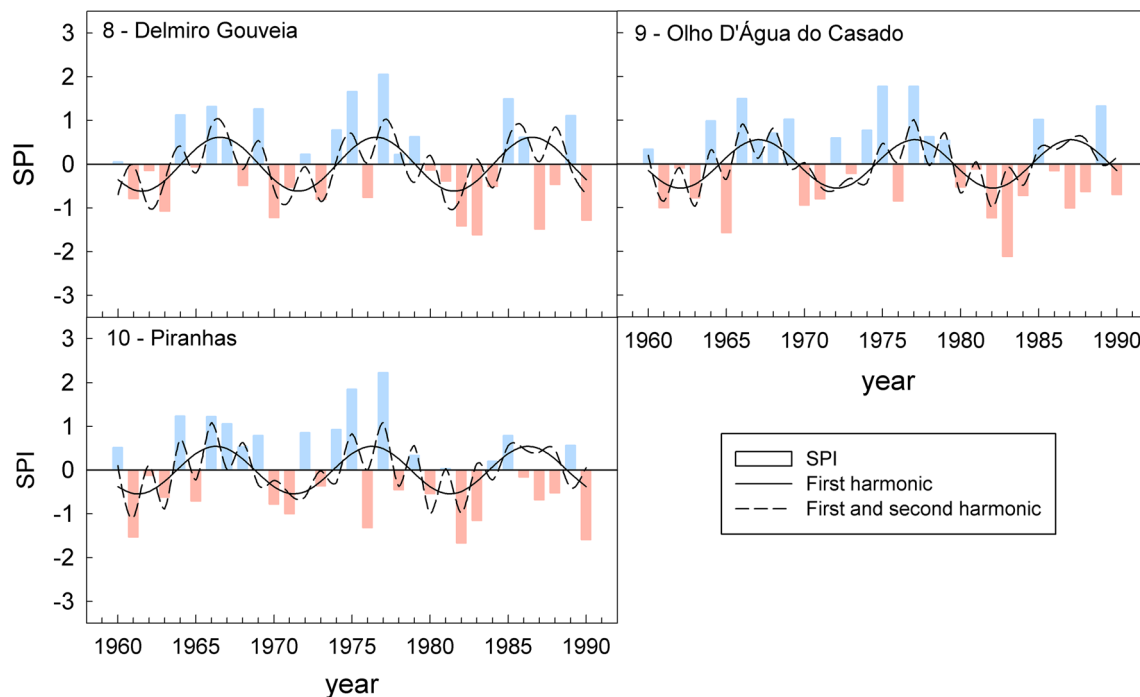**Fig. 4** Time series of SPI plotted with the first two harmonics for stations from group G_1

1989–1990) were more frequently associated with *positive* signs of AITG and ENSO, while periods with positive SPI (1985–1989) were correlated with negative AITG and ENSO indexes.

Anomalies of rainfall around the globe related to ENSO can be modulated by PDO. For example, some studies have found that ENSO and PDO have a combined effect on the distribution of anomalies of rainfall. This relationship can be constructive, with strong and well defined anomalies when ENSO and PDO have the same phase, or destructive, when both modes are out of phase (Gershunov and Barnett 1998; Wang et al. 2014). In the tropics, the most important influence of ENSO is on the sign of the vertical wind velocity associated with a Walker circulation. The Walker circulation associated with ENSO creates strong divergence/convergence of water vapor when in phase with the

PDO and weak divergence/convergence when out of phase. According to Wang et al. (2014), the phases of PDO associated with PDSI have shown strong global changes in wet/dry land conditions during winter when ENSO occurs concurrently with a warm phase of the PDO. According to that study, ENSOs out of phase with the PDO were related to weak changes in wet/dry land conditions. On the other hand, PDO have become negative in the last decades, generating more events of La Niña, which induce wet areas to become wetter and dry areas to become drier.

The second pattern is related to the stations with periods of 5 years (station 17) or 15 years (stations 12, 21, 25— Figs. 7, 8), which were located in the central part of the state, next to the transition to the highlands in the northeastern part of the state (Fig. 1). It is difficult to establish a pattern regarding the phases for those stations, since there

Fig. 5 Time series of SPI plotted with the first two harmonics for stations from group G_2

is only one with a period of 5 years, and the ones with periods of 15 years have mismatched angles of 0°, 90° or 330° (Fig. 2). It is likely that the heterogeneity in phases and periods in this region are due to the effects of the topography, such as valley-mountain circulations, which makes it difficult to compare the patterns of rainfall with other regions of the state. Indeed, a study of rainfall over the Basin of Mundaú River, where these stations are located, has shown multiscale influences related to ENSO and PDO (Da Silva et al. 2010).

The last pattern was associated with the stations on the northern coastal region with a harmonic of 10 years and phase angle of $\approx 190°$, which corresponded to 5 years (stations 26, 32, 33, 34—Fig. 9). While the stations of patterns 1–3 (Figs. 4, 5, 6) had a pattern associated with the PDO and/or ENSO, the positive SPI for stations in Fig. 9 was not related to the PDO or ENSO. Based on the harmonic analysis, periods with higher occurrence of positive SPI (1963–1967, 1973–1977 and 1983–1987) were concurrent with periods with negative AITG. However, negative values of SPI were correlated with negative values of AITG and ENSO during periods of cold PDO (1960–1962, 1968–1972). The relationships observed between SPI and the modes of variability, for each pattern of harmonics, was summarized in Table 2.

The relationships presented in Table 2 were also found in many other studies of rainfall variability over other parts of NEB. Hastenrath and Heller (1977)—using time series of rainfall from 1912 to 1958 over the northern part of

NEB—have found that dry years coincided with positive anomalies of SST over North Atlantic and East Tropical Pacific, while negative anomalies in those regions were related to years with rainfall above the average. The same relationship between positive AITG and dry years was described by Moura and Shukla (1981), for two stations in the North of NEB, and by Rao et al. (1993), for the eastern part of NEB. The effects of AITG on rainfall over NEB were reported by Nobre and Shukla (1996) to be out of phase between the northern and southern parts of the region: dry years over the north NEB were preceded by wet years over the southern part. Regarding the influence of both AITG and ENSO on rainfall in the region, Pezzi and Cavalcanti (2001) found that dry years (negative anomaly of rainfall) were related to both positive AITG and ENSO.

The relationship for warm PDO and harmonic of 10 years described in this work is in agreement with works of SST over the tropical Atlantic (Moura and Shukla 1981; Harzallah et al. 1996), which observed that the positive AITG influences the meridional position of a Hadley cell, causing the subsidence part of the cell to be located over the NEB, reducing evaporation, cloud formation and rainfall. Conversely, the negative AITG is associated with favorable conditions for evaporation and rainfall.

The influence of PDO on rainfall anomalies found here has been reported before in other studies about NEB. Andreoli and Kayano (2005), using time series of rainfall and reanalysis data, found that—during a warm PDO phase—negative rainfall anomalies are associated with
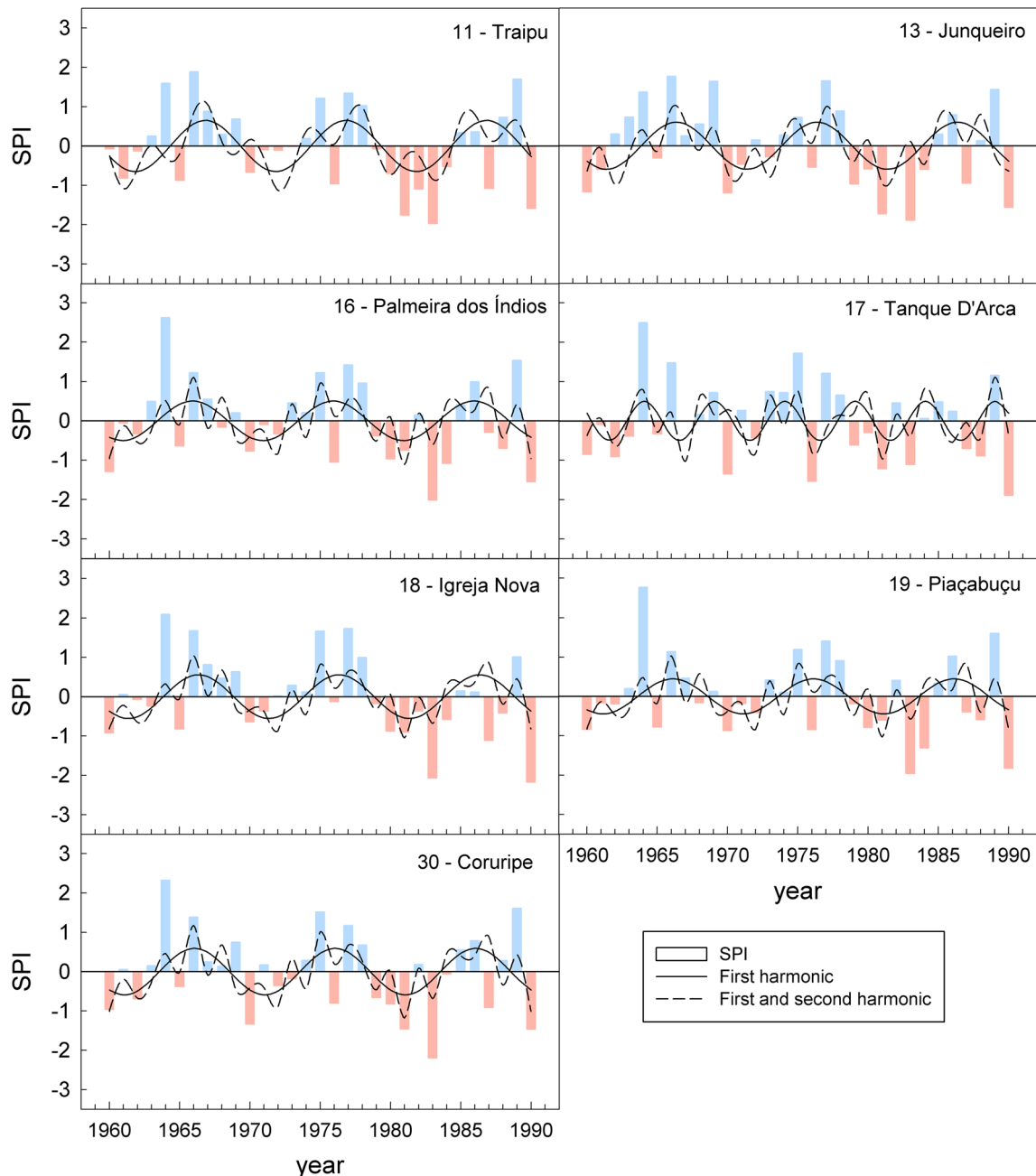
Fig. 6 Time series of SPI plotted with the first two harmonics for stations from group G_3

both a cyclone positioned over Central and Northeast Brazil and a weak anti-cyclone over Southeast South America. In addition, Kayano and Andreoli (2007) observed that between November and April the intensity of teleconnections related to ENSO increase when PDO and ENSO have the same sign, and vice versa. In a study using a global circulation model (GCM) and observational data for the austral summer also confirmed that negative anomalies of rainfall over North NEB are associated with both positive PDO and ENSO (Silva et al. 2011). Finally,

Lucena et al. (2011) used time series of anomalies of rainfall together with simulations from a GCM and divided the area of NEB in three sub-regions: north (NNEB), south (SNEB) and east (ENEB). The stations of groups G_1 and G_2 from this work were located in SNEB while ENEB contained the groups G_3, G_4 and G_5. The authors found that negative anomalies of rainfall were related to positive ENSO or AITG, in agreement with other works. However, during La Niña years NNEB and ENEB regions had two patterns: (1) during a cold PDO and negative AITG, more
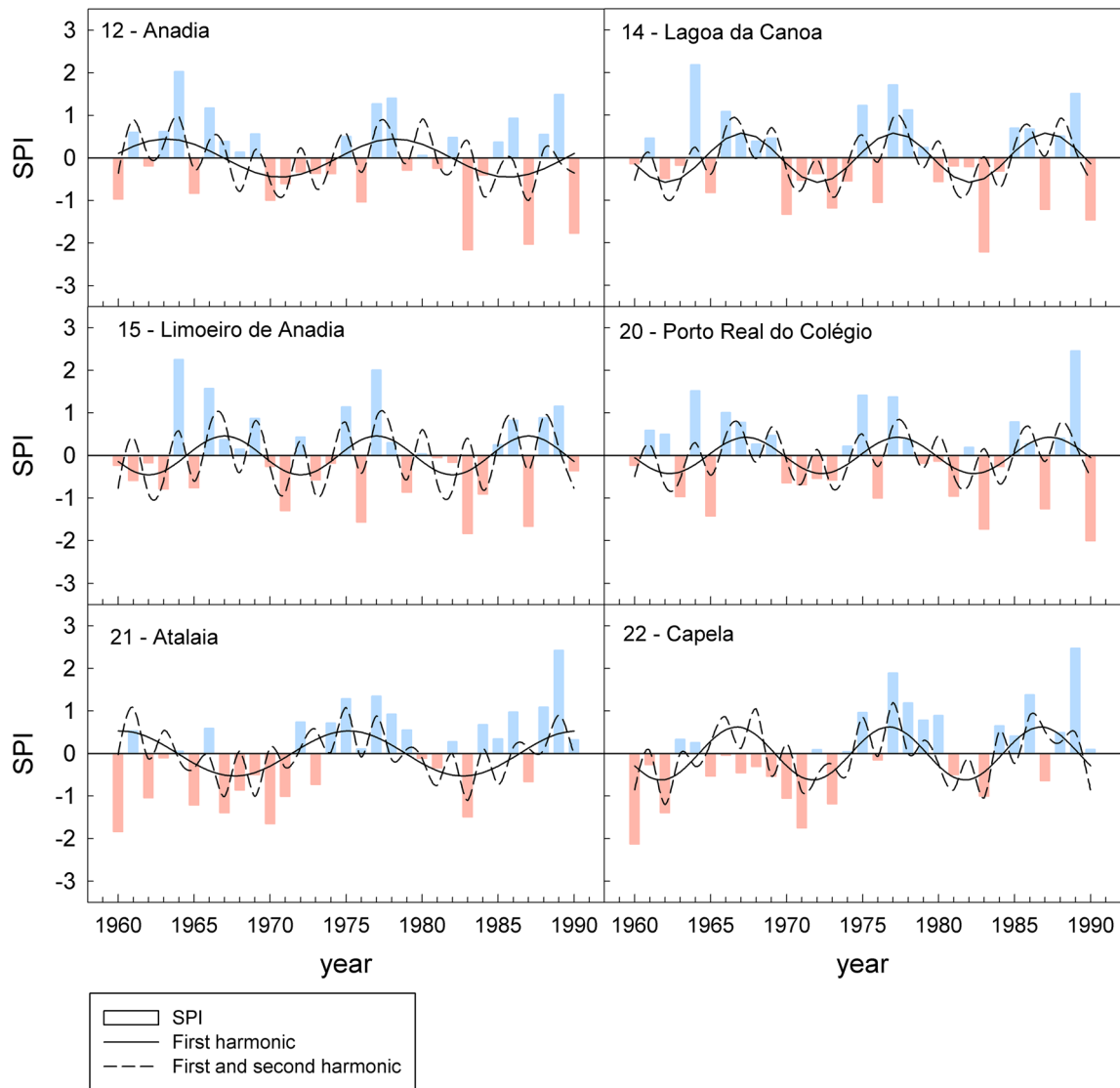
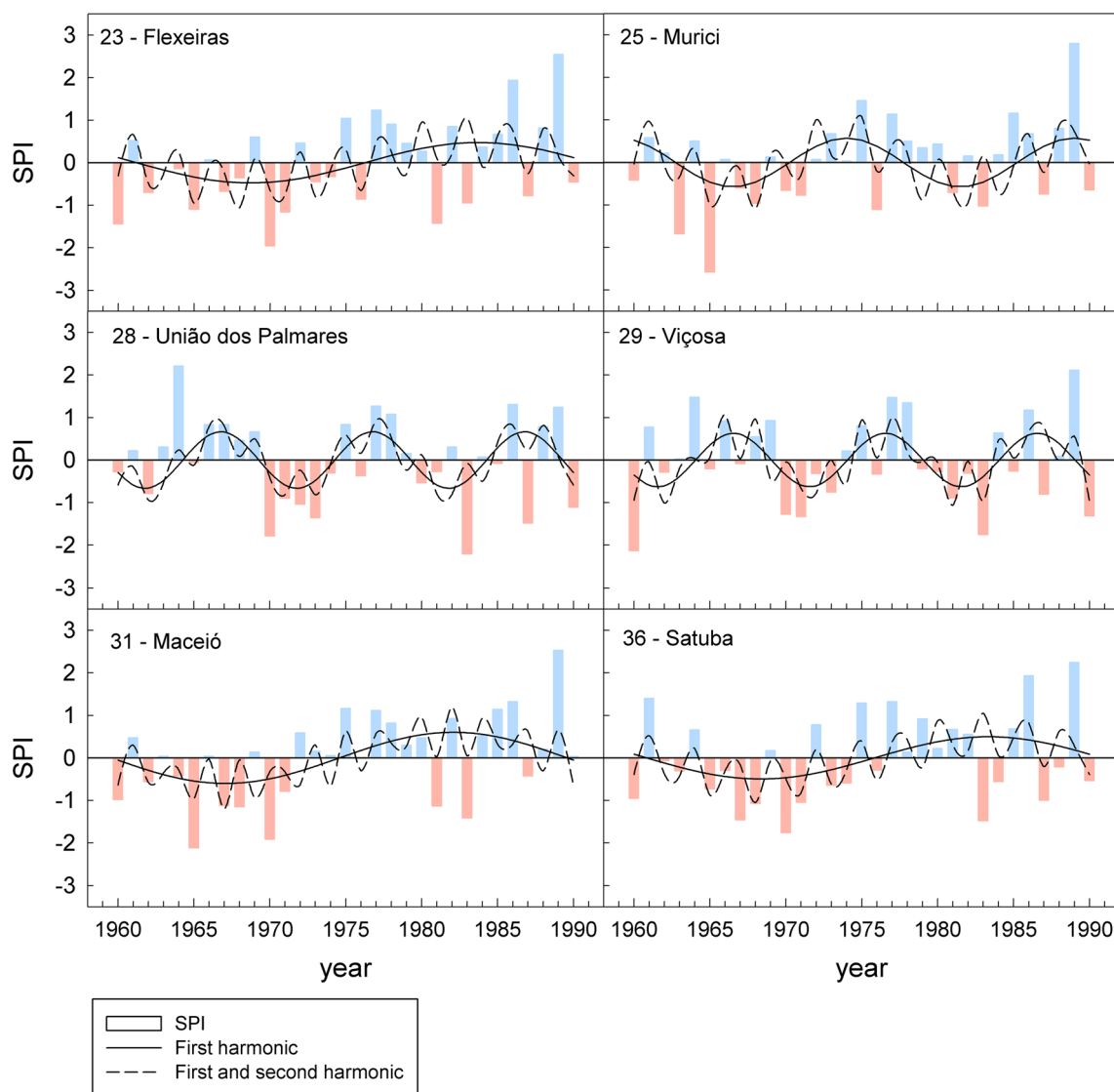**Fig. 7** Time series of SPI plotted with the first two harmonics for stations from group G_4 (part 1)

negative anomalies of rainfall were observed; (2) during a warm PDO and positive AITG, more positive anomalies of rainfall. This pattern is similar to the pattern observed for the stations with the harmonic of 10 years. For the sub-region SNEB, El Niño (La Niña) years coincided with positive (negative) anomalies of rainfall, similar to the pattern observed in this study for the harmonic of 10 years.

The results reported in Lucena et al. (2011) for different sub-regions in NEB support the grouping of stations for Alagoas state reported in (Lyra et al. 2014) and also the influence of different harmonics in areas of the state. The stations of groups G_1 to G_4, and G_5 have characteristics similar to the sub-regions SNEB and ENEB, respectively. Even a state with small area relative to NEB can have different responses to climatic modes if it is located in the

borders of large-scale regions influenced by the SST of Atlantic or Pacific oceans.

4 Conclusions

Harmonic analysis was used with time series of SPI (1960–1990) calculated using records from 33 rain gage stations in the state of Alagoas, northeast of Brazil. Two harmonics explained the most part of variability of SPI in the majority of stations. The first harmonic had a period of 10–15 years, which was most likely associated with the period of the AITG. The second harmonic had a period of 2–3 years, similar to the variability of ENSO. These results are in agreement with other studies which associated the
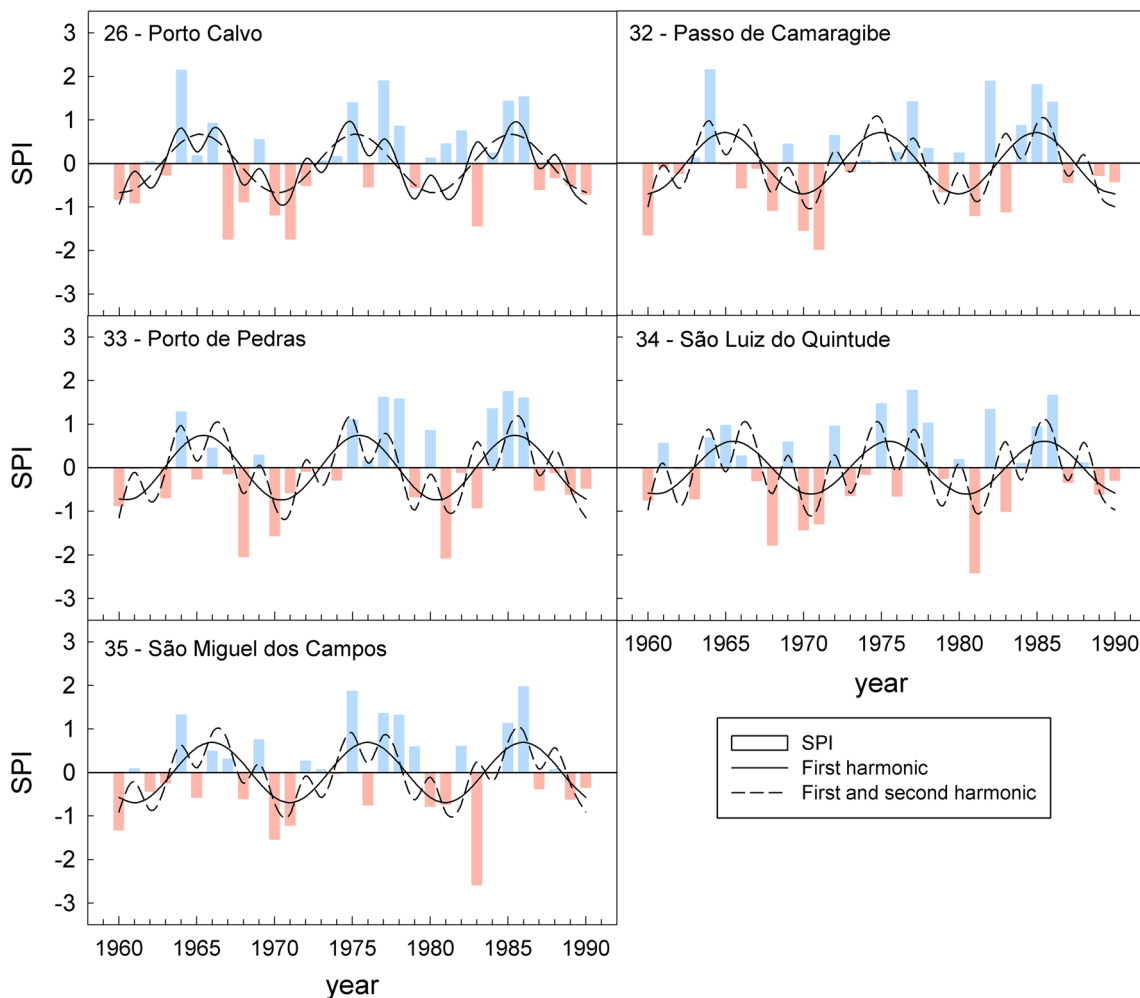
Fig. 8 Time series of SPI plotted with the first two harmonics for stations from group G$_4$ (part 2)

effects of ENSO and the Atlantic SST with rainfall over the northeast of Brazil. This study demonstrated that those influences occur in different time scales and can be significantly different even within the area of a relatively small state such as Alagoas. The proximity to the coast or the influence of the topography greatly influenced the trends and frequency of occurrence of rainfall and values of SPI.

It is well known that the combined phases of PDO, AITG and ENSO influence the displacement of subtropical anticyclones over the North and South Atlantic, which in turn affect the ITCZ, the easterly wave disturbances, the upper tropospheric cyclonic vortex and other meteorological systems associated with rainfall in every region of South America. To better understand the peculiarities of rainfall in each region, one must take into account the

influence of meteorological systems and other synoptic events, which will be considered in future works for this state. Longer time series will also be needed to assess the influence of long-term harmonics, such as the PDO, which could not be considered in this analysis due to the time series length.

The harmonic analysis is a powerful tool to identify the principal modes of variability of SPI. Although the magnitude of SPI is underestimated in some cases, this tool significantly increases the knowledge of the main drivers of rainfall and droughts in the region. The success of such analysis depends on long time series of rainfall, so that long-term trends can be identified with more confidence in the time series. The analysis presented in this study can be applied to other regions or climates. However, it is essential that the dataset is spatially extensive, covering the most

Fig. 9 Time series of SPI plotted with the first two harmonics for stations from group G₅

Table 2 Summary of relationships between positive and negative SPI and the modes of variability (PDO, AITG and ENSO)

PDO	Harmonic	SPI > 0	SPI < 0
Cold	10 years, phase 6–7	AITG (+) and ENSO (+)	AITG (−) and ENSO (−)
	15 and 30 years		AITG (−) and ENSO (−)
	10 years, phase 5	AITG (−) and ENOS (−)	AITG (−) and ENSO (−)
Warm	10 years, phase 6–7	AITG (−)	AITG (+) and ENSO (+)
	15 and 30 years	AITG (+) and ENSO (+)	
	10 years, phase 5	AITG (−)	AITG (+)

significant areas of interest, and also temporally regular, so that the characterization of trends is not affected by gaps in the data.

Finally, a descriptive analysis that shows the variability and trends of droughts is crucial not only for economic purposes (e.g., agricultural planning, civil defense, hydropower generation and weather forecast), especially in a poor state like Alagoas, but also for the formulation of public policies to address the negative impacts of such extreme events in the long-run.

References

Allen RG, Pereira LS, Raes D, Smith M (1998) Crop evapotranspiration—guidelines for computing crop water requirements, vol

56. FAO Food and Agriculture Organization of the United Nations, Rome, p 300

Alley WM (1984) The palmer drought severity index: limitations and assumptions. J Climate Appl Meteorol 23:1100–1109

Alves JMB, Repelli CA (1992) Variabilidade Pluviométrica no Setor Norte do Nordeste e os Eventos El Niño-Oscilação Sul (ENOS). Revista Brasileira de Meteorologia 7:583–592

ANA (2010) Agência Nacional de Águas

Andreoli RV, Kayano MT (2005) ENSO-related rainfall anomalies in South America and associated circulation features during warm and cold Pacific decadal oscillation regimes. Int J Climatol 25:2017–2030. doi:10.1002/joc.1222

Andreoli RV, Kayano MT (2007) A Importância relativa do Atlântico Tropical Sul e Pacífico Leste na variabilidade de Precipitação do Nordeste do Brasil. Revista Brasileira de Meteorologia 22:63–74

Andreoli RV, Kayano MT, Guedes RL, Oyama MD, Alves EMAS (2004) A Influência da Temperatura da Superfície do Mar dos Oceanos Pacífico e Atlântico na variabilidade de precipitação em Fortaleza. Revista Brasileira de Meteorologia 19:113–122

Bombardi RJ, Carvalho LMV (2011) The South Atlantic dipole and variations in the characteristics of the South American Monsoon in the WCRP-CMIP3 multi-model simulations. Clim Dyn 36:2091–2102. doi:10.1007/S00382-010-0836-9

Cañón J, González J, Valdés J (2007) Precipitation in the Colorado River Basin and its low frequency associations with PDO and ENSO signals. J Hydrol 333:252–264. doi:10.1016/j.jhydrol.2006.08.015

Cavalcanti AS (2009) Avaliações de padrões atmosféricos associados à ocorrência de chuvas extremas no litoral da região Nordeste do Brasil: Aspectos numéricos na previsão operacional do tempo. PhD thesis, COPPE/UFRJ, COPPE/Universidade Federal do Rio de Janeiro. p 236

Cavalcanti IFA (2012) Large scale and synoptic features associated with extreme precipitation over South America: a review and case studies for the first decade of the 21st century. *Atmospheric Research* 118:27–40. doi:10.1016/J.Atmosres.2012.06.012

Chang P, Link J, Hong L (1997) A decadal climate variation in the tropical Atlantic Ocean from thermodynamic air-sea interactions. Nature 385:516–518

Da Silva DF, Sousa FAS, Kayano MT (2010) Escalas temporais da variabilidade pluviométrica na bacia hidrográfica do rio Mundaú. Revista Brasileira de Meteorologia 25:324–332

Dai A, Trenberth KE, Karl TR (1998) Global variations in droughts and wet spells: 1900–1995. Geophys Res Lett 25:3367–3370

Dai A, Trenberth KE, Qian T (2004) A global dataset of palmer drought severity index for 1870–2002: relationship with soil moisture and effects of surface warming. J Hydrometeorol 5:1117–1130. doi:10.1175/jhm-386.1

Dantas MS (2008) Análise espectral de padrões-gradiente de séries temporais curtas. Master's, INPE-15676-TDI/1450, Instituto Nacional de Pesquisas Espaciais—INPE, p 157

de Souza EB, Kayano MT, Ambrizzi T (2005) Intraseasonal and submonthly variability over the Eastern Amazon and Northeast Brazil during the autumn rainy season. Theoret Appl Climatol 81:177–191. doi:10.1007/s00704-004-0081-4

Duarte RS, 2001: Seca, Pobreza e Políticas Públicas no Nordeste do Brasil. *Pobreza, desigualdad social y ciudadanía: Los límites de las políticas sociales en América Latina*, A Ziccardi, Ed., CLACSO, Buenos Aires, Argentina, pp 425–440

Fang X, Wang A, Fong S, Lin W, Liu J (2008) Changes of reanalysis-derived Northern Hemisphere summer warm extreme indices during 1948–2006 and links with climate variability. Global Planet Change 63:67–78

FAO (2010) Food and Agriculture Organization

Gershunov A, Barnett TP (1998) Interdecadal modulation of ENSO teleconnections. Bull Am Meteorol Soc 79:2715–2725. doi:10.1175/1520-0477(1998)079<2715:IMOET>2.0.CO;2

Gois G, Souza JL, Silva PRT, Oliveira-Júnior JF (2005) Caracterização da desertificação no estado de Alagoas utilizando variáveis climáticas. Revista Brasileira de Meteorologia 20:301–314

Gonçalves GR (2000) As secas na Bahia do século XIX. Master's thesis, Faculdade de Filosofia e Ciências Humanas, Universidade Federal da Bahia, p 169

Goyal MK (2014) Statistical analysis of long term trends of rainfall during 1901–2002 at Assam, India. Water Resour Manage 28:1501–1515

Grimm AM, Barros VR, Doyle ME (2000) Climate variability in Southern South America associated with El Niño and La Niña events. J Clim 13:35–58. doi:10.1175/1520-0442(2000)013<0035:cvissa>2.0.co;2

Harzallah A, Rocha de Aragão JO, Sadourny R (1996) Interannual rainfall variability in North–East Brazil: observation and model simulation. Int J Climatol 16:861–878

Hastenrath S (2012) Exploring the climate problems of Brazil's Nordeste: a review. Clim Change 112:243–251. doi:10.1007/S10584-011-0227-1

Hastenrath S, Heller L (1977) Dynamics of climatic hazards in Northeast Brazil. Quart J Royal Meteorol Soc 103:77–92. doi:10.1256/Smsqj.43504

IBGE (2006) Instituto Brasileiro de Geografia e Estatística, Censo Agropecuário. http://www.ibge.gov.br/home/estatistica/economia/agropecuaria/censoagro. Accessed 19 May 2016

Kane RP (2001) Limited effectiveness of El Niño in causing droughts in NE Brazil and the prominent role of Atlantic parameters. Revista Brasileira de Geofísica 19:231–236

Kayano MT, Andreoli RV (2007) Relations of South American summer rainfall interannual variations with the Pacific Decadal Oscillation. Int J Climatol 27:531–540. doi:10.1002/joc.1417

Kayano MT, Andreoli RV, Ferreira de Souza RA (2013) Relations between ENSO and the South Atlantic SST modes and their effects on the South American rainfall. Int J Climatol 33:2008–2023. doi:10.1002/joc.3569

Kite G (1988) Frequency and risk analyses in hydrology. Water Resourcers Publications, Littleton, p 257

Lohani VK, Loganathan GV (1997) An early warning system for drought management using the Palmer drought index. J Am Water Resour Assoc 33:1375–1386. doi:10.1111/J.1752-1688.1997.Tb03560.X

Lucena DB, Filho MFG, Servain J (2011) Avaliação do impacto de eventos climáticos extremos nos oceanos Pacífico e Atlântico sobre a estação chuvosa no Nordeste do Brasil. Revista Brasileira de Meteorologia 26:297–312

Lyra GB, Garcia BIL, Piedade SMS, Sediyama GC, Sentelhas PC (2006) Regiões homogêneas e funções de distribuição de probabilidade da precipitação pluvial no estado de Táchira, Venezuela. Pesquisa Agropecuaria Brasileira 41:202–215

Lyra GB, Oliveira-Júnior JF, Zeri M (2014) Cluster analysis applied to the spatial and temporal variability of monthly rainfall in Alagoas state, Northeast of Brazil. Int J Climatol 34:3546–3558. doi:10.1002/joc.3926

Malik K (2013) Human development report 2013—the rise of the south: human progress in a diverse world. Online at http://hdr.undp.org/en/2013-report, p 216

Mantua NJ, Hare SR, Zhang Y, Wallace JM, Francis RC (1997) A Pacific interdecadal climate oscillation with impacts on salmon production. Bull Am Meteorol Soc 78:1069–1079. doi:10.1175/1520-0477(1997)078<1069:Apicow>2.0.Co;2

Marengo J, Bernasconi M (2015) Regional differences in aridity/drought conditions over Northeast Brazil: present state and future projections. Clim Change 129:103–115. doi:10.1007/s10584-014-1310-1

McKee TB, Doesken NJ, Kleist J (1993) The relationship of drought frequency and duration to time scales. Proceedings of the 8th Conference on Applied Climatology, Boston, MA, USA, 179-184

McKee TB, Doesken NJ, Kleist J, 1995: Drought monitoring with multiple time scales. Proceedings of the 9th Conference on Applied Climatology, Dallas 233–236

Menezes HEA, Brito JD, Santos CD, Silva LD (2008) A relação entre a temperatura da superfície dos oceanos tropicais e a duração dos veranicos no Estado da Paraíba. Revista Brasileira de Meteorologia 23:152–161

Molion LCB, Bernardo SO (2002) Uma revisão da dinâmica das chuvas no Nordeste Brasileiro. Revista Brasileira de Meteorologia 17:1–10

Molion LCB, Lucio PS (2013) A note on Pacific Decadal Oscillation, El Nino Southern Oscillation, Atlantic Multidecadal Oscillation and the Intertropical Front in Sahel, Africa. Atmospheric and Climate Sciences 3:269–274. doi:10.4236/acs.2013.33028

Moreira EE, Martins DS, Pereira LS (2015) Assessing drought cycles in SPI time series using a Fourier analysis. Natural Hazards and Earth System Science 15:571–585. doi:10.5194/nhess-15-571-2015

Moura AD, Shukla J (1981) On the dynamics of droughts in northeast Brazil—observations, theory and numerical experiments with a general-circulation model. J Atmos Sci 38:2653–2675. doi:10.1175/1520-0469(1981)038<2653:Otdodi>2.0.Co;2

Nicholson SE (1997) An analysis of the ENSO Signal in the tropical Atlantic and western Indian Oceans. Int J Climatol 17:345–375. doi:10.1002/(sici)1097-0088(19970330)17:4<345:aid-joc127>3.0.co;2-3

Nobre P, Shukla J (1996) Variations of sea surface temperatures, wind stress, and rainfall over the tropical Atlantic and south American. J Clim 9:2464–2479

Oliveira-Júnior JF, Lyra G, Gois G, Brito TT, Moura NSH (2012) Análise de homogeneidade de séries pluviométricas para determinação do índice de seca IPP no estado de Alagoas. Floresta e Ambiente 19:101–112. doi:10.4322/floram.2012.011

Palmer WC (1965) Meteorological drought. Research Paper 45. Department of Commerce Weather Bureau, Washington, p 58

Panthou G, Vischel T, Lebel T (2014) Recent trends in the regime of extreme rainfall in the Central Sahel. Int J Climatol. doi:10.1002/joc.3984

Penalba OC, Vargas WM (2004) Interdecadal and interannual variations of annual and extreme precipitation over central-northeastern Argentina. Int J Climatol 24:1565–1580

Pezzi LP, Cavalcanti IFA (2001) The relative importance of ENSO and tropical Atlantic sea surface temperature anomalies for seasonal precipitation over South America: a numerical study. Clim Dyn 17:205–212. doi:10.1007/s003820000104

Rao VB, Hada K (1990) Characteristics of rainfall over Brazil—annual variations and connections with the southern oscillation. Theor Appl Climatol 42:81–91. doi:10.1007/Bf00868215

Rao VB, de Lima MC, Franchito SH (1993) Seasonal and interannual variations of rainfall over Eastern Northeast Brazil. J Clim 6:1754–1763. doi:10.1175/1520-0442(1993)006<1754:saivor>2.0.co;2

Rasmusson EM, Carpenter TH (1982) Variations in tropical sea surface temperature and surface wind fields associated with the Southern Oscillation/El Niño. Mon Weather Rev 110:354–384

Santos DN, da Silva VPR, Sousa FAS, Silva RA (2010) Estudo de alguns cenários climáticos para o Nordeste do Brasil. Revista Brasileira de Engenharia Agrícola e Ambiental 14:492–500

Servain J (1991) Simple climatic indices for the tropical Atlantic Ocean and some applications. J Geophy Res Oceans 96:15137–15146. doi:10.1029/91JC01046

Servain J, Clauzet G, Wainer IC (2003) Modes of tropical Atlantic climate variability observed by PIRATA. Geophys Res Lett 30:8003. doi:10.1029/2002GL015124

Silva DF, Sousa FAS, Kayano MT (2009) Uso de IAC e ondeletas para análise da influência das multi-escalas temporais na precipitação da bacia do rio Mundaú. Revista de Engenharia Ambiental 6:180–195

Silva DF, Sousa FAS, Kayano MT (2010) Escalas temporais da variabilidade pluviométrica na bacia hidrográfica do Rio Mundaú. Revista Brasileira de Meteorologia 25:324–332. doi:10.1590/S0102-77862010000300004

Silva GAMd, Drumond A, Ambrizzi T (2011) The impact of El Niño on South American summer climate during different phases of the Pacific Decadal Oscillation. Theoret Appl Climatol 106:307–319. doi:10.1007/s00704-011-0427-7

Souza EB, Nobre P (1998) Uma Revisao Sobre O Padrão De Dipolo No Atlântico Tropical. Revista Brasileira de Meteorologia 13:31–44

Souza EB, Brabo Alves JM, Nobre P (1998) Anomalias de precipitação nos setores Norte e Leste do Nordeste Brasileiro em associação aos eventos do padrão de dipolo observados na Bacia do Atlântico. Revista Brasileira de Meteorologia 13:45–55

Štěpánek P, Zahradníček P, Skalák P (2009) Data quality control and homogenization of air temperature and precipitation series in the area of the Czech Republic in the period 1961–2007. Advances in Science and Research 3:23–26. doi:10.5194/asr-3-23-2009

Thom HCS (1958) A note on the gamma distribution. Mon Weather Rev 86:117–122

Torres RR, Ferreira NJ (2011) Case studies of easterly wave disturbances over northeast Brazil using the eta model. Weather Forecast 26:225–235. doi:10.1175/2010waf2222425.1

Uvo CB, Repelli CA, Zebiak SE, Kushnir Y (1998) The relationships between Tropical Pacific and Atlantic SST and Northeast Brazil Monthly Precipitation. J Clim 11:551–562. doi:10.1175/1520-0442(1998)011<0551:trbtpa>2.0.co;2

Vegas-Vilarrubia T, Sigro J, Giralt S (2012) Connection between El Nino-Southern Oscillation events and river nitrate concentrations in a Mediterranean river. Sci Total Environ 426:446–453. doi:10.1016/j.scitotenv.2012.03.079

Vicente-Serrano SM, Beguería S, López-Moreno JI, García-Vera MA, Stepanek P (2010) A complete daily precipitation database for northeast Spain: reconstruction, quality control, and homogeneity. Int J Climatol 30:1146–1163. doi:10.1002/joc.1850

Wang S, Huang J, He Y, Guan Y (2014) Combined effects of the Pacific Decadal Oscillation and El Niño-Southern Oscillation on Global Land Dry-Wet Changes. Sci Rep. doi:10.1038/srep06651

Wilks DS (1995) Statistical methods in the atmospheric sciences: an introduction, vol 59. Academic Press, San Diego, p 467

WMO (2006) Guide to meteorological instruments and methods of observation. Preliminary seventh edition, WMO-No. 8. World Meteorological Organization, Geneva, p 569

Wolter K (1987) The southern oscillation in surface circulation and climate over the tropical Atlantic, eastern Pacific, and Indian Oceans as captured by cluster analysis. J Climate Appl Meteorol 26:540–558. doi:10.1175/1520-0450(1987)026<0540:tsoisc>2.0.co;2

Wolter K (2016) Multivariate ENSO Index (MEI)—NOAA Earth System Research Laboratory—Physical Sciences Division. National Atmospheric and Oceanic Administration. [Available online at http://www.esrl.noaa.gov/psd/enso/mei/.]

Wolter K, Timlin MS (2011) El Niño/Southern Oscillation behaviour since 1871 as diagnosed in an extended multivariate ENSO index (MEI.ext). Int J Climatol 31:1074–1087

Zhang Y, Wallace JM, Battisti DS (1997) ENSO-like Interdecadal Variability: 1900–93. J Clim 10:1004–1020